

# A Comparative Study of Two Different SnO<sub>2</sub>:F-coated Glass Substrates for CdTe Solar Cells

Eun Seok Cha · Young Min Ko · Yong Woo Choi · Gyu Chan Park · Byung Tae Ahn\*

Dept. of Materials Science and Engineering, Korea Advanced Institute of Science and Technology, 291 Daehak-ro, Yuseong-gu, Daejeon 34141, Republic of Korea

**ABSTRACT:** Two different fluorine-doped tin oxide (FTO)-coated glass substrates were investigated to find better suitability for CdTe solar cells. Substrate A consisted of FTO (300 nm)/SiO<sub>2</sub> (24 nm)/intrinsic SnO<sub>2</sub> (30 nm)/borosilicate glass (2.2 mm), and substrate B consisted of FTO (700 nm)/intrinsic SnO<sub>2</sub> (30nm)/borosilicate glass (1.8 mm). The overall thickness of the FTO/glass substrates was about 2.5 mm. The total light transmittance of substrate B was much higher than that of substrate A throughout the whole spectral region, even though the thickness of the FTO in substrate B was twice larger than that of the FTO in the substrate A. The short-circuit current greatly increased in substrate B and the external quantum efficiency (EQE) increased over the whole wavelength range. This study shows that the diffuse optical transmittance played a key role in the large EQE value in the blue wavelength region, and the direct transmittance played a key role in the large EQE value in the red wavelength region. The higher transmittance is due to the rough surface generated by the thicker FTO on glass. The conversion efficiency of the CdTe solar cell increased from 12.4 to 15.1% in combination of rough FTO substrate and Cu solution back contact.

**Key words:** CdTe solar cells, FTO glass, Surface morphology, Diffuse optical transmittance, Short circuit current

## 1. Introduction

Recent progress by GE and First Solar reported above 20% cell efficiency<sup>1)</sup>. However, little information on the structure of the cell is known. As a result, scientific and technological progress from the academic side has so far been very limited. To achieve theoretical efficiency of above 25%, it is necessary to correctly understand the physics behind the CdTe solar cell, which has much lower efficiency. Conventional CdTe cells are fabricated on transparent-conductive-oxide (TCO) electrodes and consist of a CdS/CdTe heterojunction in which CdS is a window material and CdTe is a light absorbing material. Since the band gap of CdS is 2.4 eV and the thickness of CdS is around 200 nm, incident light with photon energies of more than 2.4 eV is absorbed and lost in the CdS window layer. As a result, the blue light is lost and the light-generated current is limited.

To reduce absorption loss in the blue wavelength region by the window material, it is necessary to increase the band gap of the window layer or reduce the thickness of the CdS layer. An increase in the band gap of the window layer was achieved by

changing the composition of the window layer to CdS:O<sup>2,3)</sup>. The reduction in the CdS thickness was achieved by introducing a highly resistive layer including SnO<sub>2</sub> and Zn<sub>2</sub>SnO<sub>4</sub> on a thin CdS layer<sup>2-4)</sup>. Previously, we introduced a highly resistive In<sub>2</sub>S<sub>3</sub> and ZnO layer on a very thin CdS buffer to increase the light transmittance and reduce the recombination current through the junction<sup>5,6)</sup>. We found that with a ZnO resistive layer the thickness of CdTe can be reduced to below 70 nm.

In addition to the CdS window layer, it is believed that the light transmission through the TCO plays an important role. The development of TCO is still a hot topic in the pursuit of higher CdTe cell performance<sup>7-9)</sup>. Conventionally, indium-tin-oxide (ITO) electrode with a resistivity value of  $2 \times 10^{-4} \Omega \cdot \text{cm}^2$  was favorable<sup>10)</sup>. With an ITO electrode, a cell with a larger area was fabricated but the efficiency was just slightly over 10%. A University of South Florida team demonstrated that the efficiency was much improved by employing a fluorine-doped tin oxide (SnO<sub>2</sub> : F, FTO) as an electrode<sup>11)</sup>. However, the details of the FTO substrate effect was not known. Since we developed a ZnO/CdS buffer layer that demonstrated high optical transmittance and low tunneling recombination<sup>6)</sup>, it is worthwhile to select various FTO substrates to investigate the role of the FTO substrate. In our experiment, we selected two FTO glass substrates purchased from two different companies and applied them to

\*Corresponding author: btahn@kaist.ac.kr

Received January, 24, 2017; Revised February, 07, 2017;

Accepted February, 09, 2017

CdTe solar cells and compared the CdTe cell performance in respect to the FTO optical transmittance.

## 2. Experimentals

The schematic cross sections of the two different FTO-coated glass substrates we selected are shown in Fig. 1. Substrate A consisted of FTO (300 nm)/ SiO<sub>2</sub> (24 nm)/ SnO<sub>2</sub> (30 nm)/ borosilicate glass (2.2 mm), purchased from Sigma-Aldrich and called FTO glass TEC 10. Substrate B consisted of FTO (700 nm)/ SnO<sub>2</sub> (30 nm)/ borosilicate glass (1.8 mm), purchased from Asahi and called TEC 7/2.2. The sheet resistances of substrate A and substrate B were approximately 10 and 7 Ω/□, respectively; consequently, the resistivities of substrate A and substrate B were  $3 \times 10^{-4}$  and  $4.9 \times 10^{-4}$  Ω · cm, respectively. The size of the

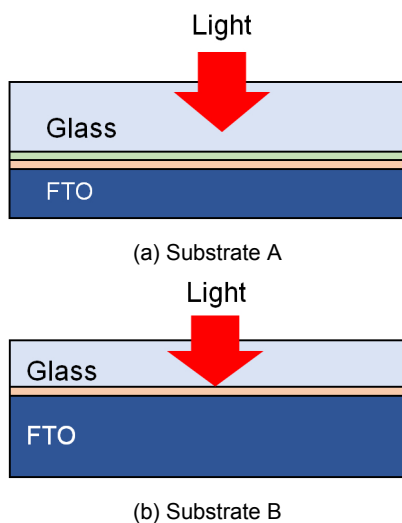


**Fig. 1.** Schematic cross sections of the two glass substrates with different FTO and glass thicknesses. Overall thickness is about 2.5 mm.

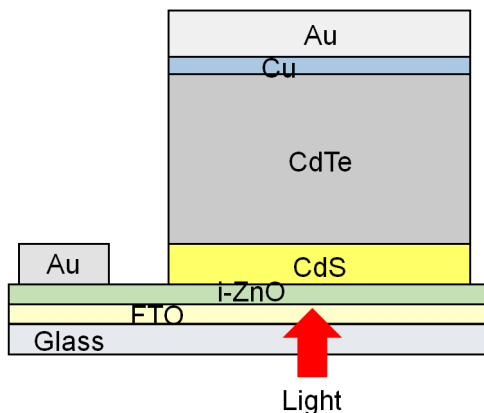


**Fig. 2.** Schematic cross sectional structure of CdTe solar cells.

FTO-coated borosilicate glass was  $2 \times 5$  cm<sup>2</sup>. Note that the resistivity of substrate B was larger than that of substrate A, indicating that the carrier concentration was smaller in substrate B than in substrate A. The substrates were cleaned ultrasonically in acetone and ethanol for 15 minutes and dried in a forced convection oven at 70°C for 15 minutes.

CdTe solar cells were fabricated in a FTO/ZnO/CdS/CdTe superstrate configuration. The schematic cross section of the CdTe cell is shown in Fig. 2. A 100-nm thick ZnO buffer layer was deposited on the FTO substrate at 100°C by RF-sputtering of a 4-inch ZnO target at a sputtering power of 135 W. The base pressure and working pressure were  $2 \times 10^{-6}$  and  $2 \times 10^{-3}$  Torr, respectively. Then, a 70-nm thick CdS layer was deposited on the ZnO-coated sample by immersing the substrate into a reaction beaker filled with distilled water, Cd(CH<sub>3</sub>COO)<sub>2</sub>, NH<sub>4</sub>(CH<sub>3</sub>COO), and CH<sub>4</sub>N<sub>2</sub>S and by increasing the reaction beaker to 85°C.

The CdS/ZnO-coated sample was inserted into a close-space sublimation (CSS) chamber, in which the distance between the CdTe source plate and the sample plate was 2 mm. The CSS chamber was pumped down to 10 mTorr and filled with oxygen to 5 Torr. The source temperature and sample temperature were 620 and 575°C, respectively. A 4-μm-thick CdTe layer was deposited with a growth rate of about 1 μm/min. After CdTe deposition, the sample was dipped into a CdCl<sub>2</sub> solution and dried immediately with an N<sub>2</sub> blow gun. Then the sample was annealed at 380°C for 10 minutes in a chamber filled with 80% He + 20% O<sub>2</sub>. Following the CdCl<sub>2</sub> heat treatment, the residual CdCl<sub>2</sub> on the CdTe surface was rinsed off.

The detailed process of the p<sup>+</sup> contact on CdTe is as follows. The CdTe surface was etched by nitric phosphoric (NP) acid for 15 seconds and rinsed in water. Then, a 1-nm thick Cu metal layer was deposited on the CdTe surface at room temperature. Then the sample was annealed at 220°C for 10 minutes in N<sub>2</sub>. This contact technology is called the Cu metal contact. After the p<sup>+</sup> contact process, a mechanical scribing was performed to make cell outlines and to expose the FTO front contact. Then a 100-nm thick Au layer was deposited by thermal evaporation with a deposition rate of 2 Å/s. Finally, a second scribing was performed within the previously defined cell outline. Four CdTe solar cells with a size of  $W \times L = 1 \times 0.5$  cm<sup>2</sup> were fabricated for one glass substrate.

The optical transmittance of the FTO-coated glass substrate was characterized using UV-vis spectroscopic transmittance measurement. The morphology and layer thickness of the ZnO

and CdS films were measured using a scanning electron microscope (SEM). The photovoltaic properties of the CdTe solar cells were measured using a solar simulator at AM 1.5 one sun conditions, which was calibrated with a silicon reference cell. The external quantum efficiency (EQE) was measured using a QEX10 solar cell QE system produced by PV measurement Inc.

### 3. Results and discussion

#### 3.1 Effect of substrate type

Fig. 3 shows the cross-sectional SEM morphologies of (a) 700-nm thick FTO on a glass substrate (substrate B) and (b) CdTe/FTO/ glass configuration on substrate B. In Fig. 3a, the FTO layer on glass shows a columnar structure with a width of approximately 300 nm. A 30-nm thick SnO<sub>2</sub> layer can be seen at the FTO/glass interface. The surface of the FTO layer on substrate B is rather flat and consists of many pyramid-shaped grain surfaces. In Fig. 3b, the demarcation of the ZnO/CdS buffer layer is seen between CdTe and FTO. A pore was developed between the buffer and CdTe interface.

Fig. 4 shows the direct, diffuse, and total transmittances of the

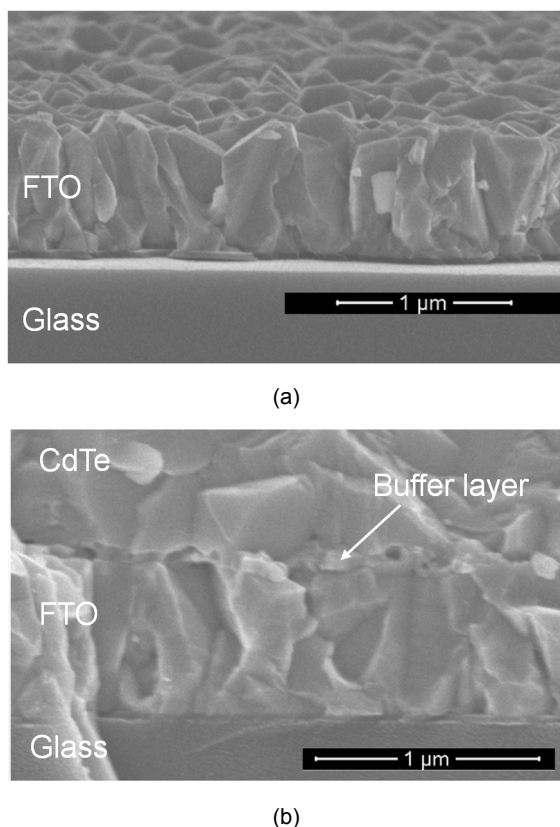


**Fig. 3.** Cross-sectional SEM images of 700-nm thick FTO on glass (a) and the CdTe/FTO/glass interface (b).

two different substrates: substrate A and substrate B. The notable result is that the total transmittance of substrate B is much higher than that of substrate A, both in the blue wavelength region and also in the red wavelength region.

In the blue wavelength region, the direct transmittance of substrate B is smaller than that of substrate A. The thicknesses of FTO in substrate A and substrate B are 300 and 700 nm, respectively. Therefore, it is expected that the absorption loss by free carrier scattering is greater in substrate B than in substrate A. However, note that the diffuse transmittance of substrate B is much bigger than that of substrate A.

The total transmittance is the sum of direct transmittance and diffuse transmittance. It is clearly seen that the total transmittance of substrate B is much larger than that of the substrate in the blue wavelength region. At around 400 nm, the wavelength region, the total transmittance value of substrate B is about 97%, while the value of substrate A is 82%. The maximum difference is a 15% point at 400 nm. The difference decreased as the wavelength increased to higher than 400 nm. The main contribution of the high transmittance in substrate B is the great increase in the diffuse transmittance.

The SEM surface morphology shown in Fig. 3 shows that the FTO surface has a pyramid shape that can scatter and increase the light absorption. The thicknesses of the FTO in substrate B and substrate A are 700 and 300 nm, respectively. We consider that the pyramid shape is more developed as the thickness of the FTO increases.

In the red wavelength region, the transmittance of substrate B is much larger than that of substrate A. At 790 nm, the total transmittance values of substrate A and substrate B are 76 and

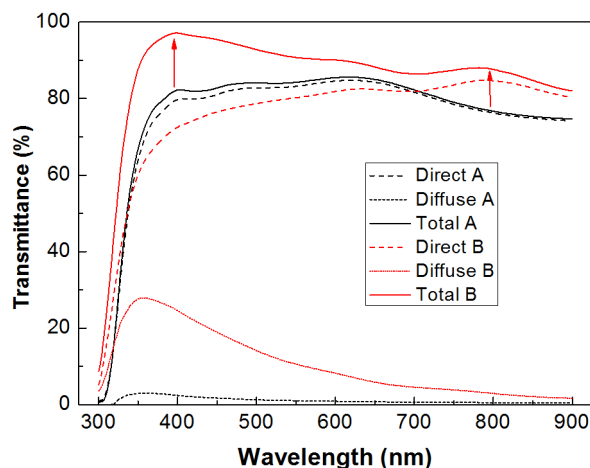


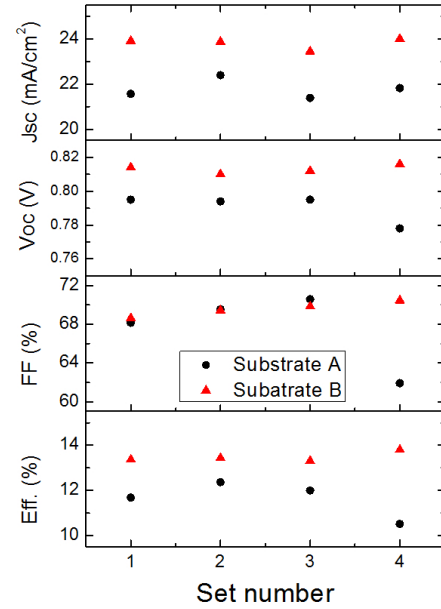
**Fig. 4.** Spectroscopic direct and diffuse transmittances of two different substrates.

88%, respectively. Substrate B showed a 12.0% point enhancement, which is a big increase. The main contribution is the increase of the direct transmittance in substrate B. Since the resistivities of substrate A and substrate B are  $3 \times 10^{-4}$  and  $4.9 \times 10^{-4} \Omega \cdot \text{cm}$ , respectively, it is clear that the carrier concentration in substrate B is smaller than in substrate A, by assuming that the carrier mobility in substrate A is similar to that in substrate B because the F-doping process was conducted by a CVD process. With the lower carrier concentration in substrate B, the light scattering is less severe in the red wavelength region, which results in the higher optical transmittance.

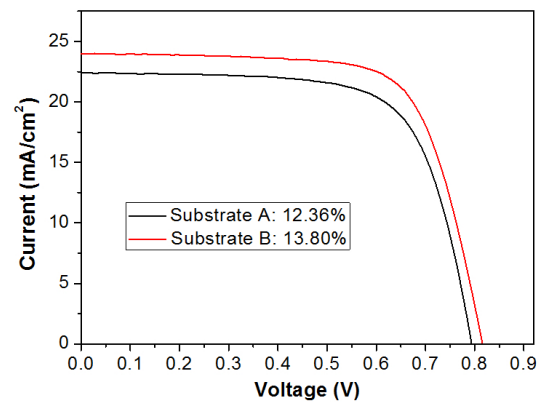
Fig. 5 shows the reproducibility of the CdTe cell performance for the two different FTO substrates. For the cell fabrication, a 100-nm thick ZnO buffer layer was deposited on the FTO substrate at 100°C by RF-sputtering and a 70-nm thick CdS layer was deposited by a CBD process at 85°C. A p+ contact was prepared by depositing a 1-nm thick Cu metal layer and annealing at 200°C for 10 minutes. The cell performance was quite reproducible even though the deposition temperature of ZnO was rather low. Note that the cell efficiency ( $\eta$ ) was consistently higher and more reproducible for the cells prepared on substrate B than on substrate A. The short-circuit current ( $J_{sc}$ ) and open-circuit voltage ( $V_{oc}$ ) of the cell on substrate B were much higher than those of the cell on substrate A, while the fill factors (FF) were similar.

Fig. 6 compares the illuminated J-V curves (a) and external quantum efficiency (EQE) curves of the best results of the CdTe cell with two different substrates. In Fig. 6(a), the  $J_{sc}$  and  $V_{oc}$  increased more for the cell on substrate B than for the cell on substrate A. The cell efficiencies of the cells on substrates A and B were 12.4 and 13.80%, respectively, a 1.4 % point increase on substrate B over that on substrate A. The photovoltaic parameters,  $J_{sc}$ ,  $V_{oc}$ , FF, shunt resistance ( $R_{sh}$ ), and series resistance ( $R_s$ ), of the cells are summarized in Table 1. Compared with the cell on substrate A, the  $J_{sc}$  and  $V_{oc}$  of the cell on substrate B increased with 16 and 3% changes, while little change was found in the FF. Therefore, the main parameter of the cell performance increase was due to the increase of the  $J_{sc}$ .

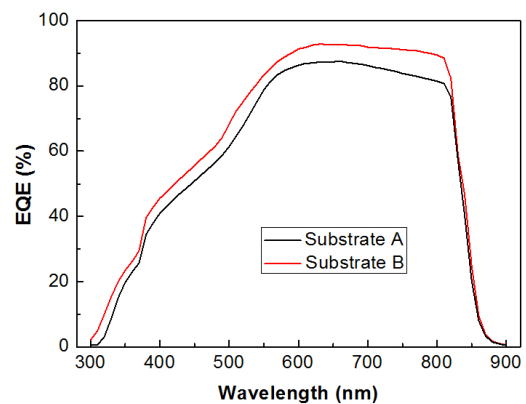
The origin of the  $J_{sc}$  increase can be inferred from the EQE curves as shown in Fig. 6(b). Note that the EQE value of the cell on substrate B is higher than that of the cell on substrate A throughout the whole spectrum range. This suggests that the increase of the  $J_{sc}$  is due to the higher transmittance of incident light through substrate B than through the substrate. The result matches well with the higher total optical transmittance through



**Fig. 5.** Efficiency variation of CdTe solar cells with a ZnO/CdS/CdTe/FTO/glass configuration. The thicknesses of ZnO and CdS are 100 and CdS 70 nm, respectively.



(a)



(b)

**Fig. 6.** Comparison of the best cells with two different substrates: 12.4% on substrate A and 13.8% on substrate B. The 600-nm thick FTO layer shows a higher efficiency than the 300-nm thick FTO layer.

**Table 1.** PV parameters of the CdTe cell with two different substrates. ZnO (100 nm)/CdS (70 nm) buffer

Substrate	Contact	$\eta$	$J_{sc}$	$V_{oc}$	FF	$R_{sh}$	$R_s$
		(%)	(mA/cm <sup>2</sup> )	(V)	(%)	( $\Omega \cdot \text{cm}^2$ )	( $\Omega \cdot \text{cm}^2$ )
A	Cu metal	12.45	22.40	0.794	70	3191	8.4
B	Cu metal	13.81	24.00	0.816	70.5	1988	9.7
		(10.9%)	(7.1%)	(2.8%)	(0.07%)		
B	Cu solution	15.06	26.11	0.82	70.3	950	1.25

substrate B than substrate A as shown in Fig. 4, which demonstrates the optical transmittance. Our result indicates that the design of the FTO layer on a glass substrate is very important in achieving higher cell performance. In particular, an appropriate surface roughness (or texturing) is necessary to increase the diffuse transmittance and the resulting total transmittance. In addition to the increase in the total transmittance, the increase in the diffuse transmittance seems to be important because it increases the pathway of the transmitted light and enhances the light absorption near the CIGS surface or near the depletion region.

### 3.2 Effect of p<sup>+</sup> contact

The biggest issue in the CdTe solar cell was development of a stable p<sup>+</sup> back contact. The most suitable method is Cu doping on CdTe, but the CdTe cell is easily degraded by Cu contamination at the CdS/CdTe junction<sup>12-14</sup>. Degradation of the cell has several reasons, among them, shunting at the CdS/CdTe interface<sup>15</sup> and light shielding through an impurity level in the CdS layer for a photon energy of 1.55 eV ( $\lambda=803$  nm)<sup>16</sup>. With the Cu contamination at the CdS/CdTe interface, the QE value near the red-wavelength region was drastically reduced<sup>16-18</sup>, which supported the light shielding by Cu contamination in CdS<sup>16</sup>. Therefore, it is imperative to reduce the Cu contamination in CdTe solar cells. For that purpose, the total amount of Cu in the back contact source should be as low as possible, while the Cu concentration at the back surface should be as high as possible for the p<sup>+</sup> contact.

For that purpose, a Cu solution was applied on the CdTe back contact instead of Cu metal<sup>14</sup>. The detailed process of the Cu-solution contact is as follows. The surface of the CdCl<sub>2</sub> heat treated CdTe film was dipped for one minute in a Cu acetate solution and dried in a 70°C oven. The solution consisted of 0.08 g Cu acetate in 100 ml DI water. Then the sample was annealed at 250°C for 10 minutes. This contact technology is called the Cu solution contact to distinguish it from the Cu metal contact technology.

**Table 2.**  $J_{sc}$  and  $V_{oc}$  of CdTe solar cells with various annealing temperatures of the Cu solution back contact

Temp. (°C)	Time (min)	JSC (mA/cm <sup>2</sup> )	VOC (V)	$J_{sc} \times V_{oc}$
180	10	23.34	0.76	17.74
200	10	24.54	0.768	18.85
220	10	24.49	0.79	19.34
250	10	24.56	0.795	19.53
270	10	23.81	0.782	18.62

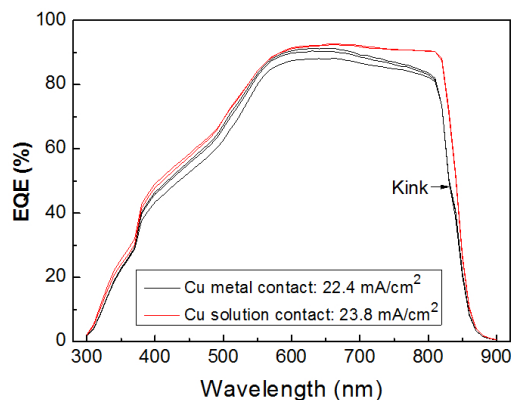
**Fig. 7.** EQE curves of the CdTe cells fabricated on the thick FTO substrate with two different Cu contact technologies. The Cu solution contact shows a higher short-circuit current than the Cu metal contact.

Table 2 summarizes the change of  $J_{sc}$ ,  $V_{oc}$ , and the  $J_{sc} \times V_{oc}$  as a function of the contact annealing temperature in the Cu-solution contact technology. It is seen that the product of  $J_{sc}$  and  $V_{oc}$  is the largest in the temperature range of 220 to 250°C. At 200°C, the  $J_{sc}$  is large but the  $V_{oc}$  is small, probably due to the poor p<sup>+</sup> contact in the back side. Table 2 reveals that both the  $J_{sc}$  and  $V_{oc}$  decreased at 270°C.

Fig. 7 shows the EQE curves of the CdTe cells fabricated on substrate B with two different p<sup>+</sup> metal contact technologies. The Cu solution contact was performed at 250°C for 10 minutes. The EQE curves of the three CdTe cells fabricated by metal contact and two Cu CdTe cells with the Cu solution contact were demonstrated. It is seen that the EQE values increased in the whole wavelength region by the Cu solution contact, especially



in the red wavelength region ( $\sim 800$  nm). The average  $J_{sc}$  values of the CdTe cells with the Cu metal contact and Cu solution contact were  $22.4$  and  $23.8$   $\text{mA}/\text{cm}^2$ , respectively.

Note that there was a kink at a wavelength of  $830$  nm ( $1.49$  eV at room temperature). The difference in the EQE values near the kink was very large. For example, the EQE values of the CdTe cells with the Cu metal contact and Cu solution contact were  $90$  and  $48\%$ , respectively. The origin of the kink was due to the formation of Cu doping into the CdS buffer layer, resulting in the formation of an acceptor energy level of  $1.49$  eV below the CdS conduction band. The energy level screened the photon energy above the  $1.49$  eV and reduced the light transmittance. The Cu migrated from the back contact to the CdS/CdTe interface<sup>6</sup>.

The other noticeable thing was that the EQE value of the CdTe cell with the Cu metal contact was much lower in the red wavelength region ( $700$ – $800$  nm) than that of the CdTe cell with the Cu solution contact. That was probably due to the formation of interstitial Cu in the bulk CdTe by the Cu migration from the Cu back contact. Since Cu had already diffused to the CdS/CdTe interface and formed Cu doping in the CdS, it is very likely that there were interstitial Cu atoms in the CdTe film. The interstitial Cu atoms acted as donors and reduced the carrier mobility, resulting in the significant reduction of the EQE value in the red wavelength region.

Fig. 8 shows the contour plot of  $V_{oc}$  of the CdTe cell on substrate B as functions of the contact annealing temperature and time for the Cu solution contact. A  $V_{oc}$  of  $0.8$  V  $V_{oc}$  was obtained in a temperature range of  $230$  to  $260^\circ\text{C}$  and in a time range of  $11$  to  $13$  minutes. The deposition temperature of the ZnO buffer layer increased from  $100$  to  $300^\circ\text{C}$  to obtain a dense layer and the  $V_{oc}$  annealed at  $250^\circ\text{C}$  increased to  $0.82$  V.

Fig. 9 shows the illuminated J-V curve of the best CdTe cells prepared on substrate B with a metal contact and Cu-solution contact. The thicknesses of ZnO and CdS were  $100$  and  $70$  nm, respectively. The best cell efficiencies of the cells with the Cu metal contact and Cu solution contact were  $13.8\%$  and  $15.1\%$ . For the  $15.1\%$  cell, the  $J_{sc}$ ,  $V_{oc}$  and FF were  $26.11$   $\text{mA}/\text{cm}^2$ ,  $0.82$  V, and  $0.70$ , respectively. The difference between the two cells were the deposition temperature of the ZnO buffer. The deposition temperatures of the  $100$ -nm thick ZnO buffer for the Cu metal contact and Cu solution contact here were  $100$  and  $300^\circ\text{C}$ . The ZnO buffer deposited at  $300^\circ\text{C}$  had a dense film and better step coverage on FTO glass. The details of the ZnO deposition temperature effect was reported in a previous study<sup>6</sup>.

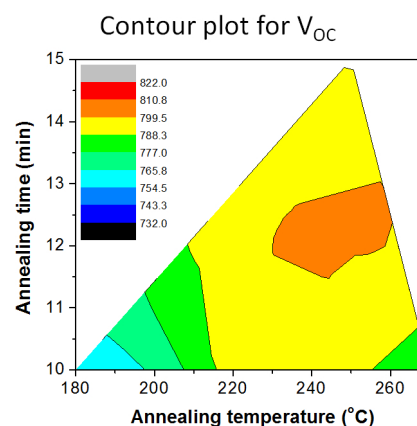


Fig. 8. Contour plot for open-circuit voltage with various annealing temperatures with a back contact using a Cu solution.

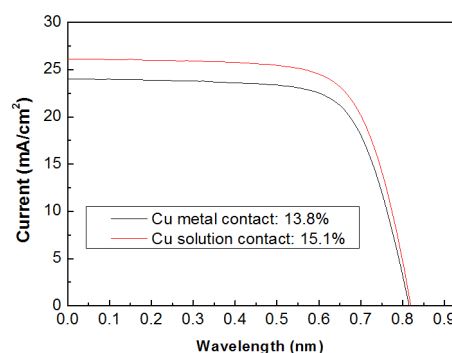


Fig. 9. The best CdTe cells on the FTO glass.

We have seen that the selection of the FTO substrate greatly affects the light transmittance. The FTO layer with a  $700$  nm thickness had better light transmittance than that with  $300$  nm. The main increase of the transmittance was the large increase of the diffuse transmittance in the blue-wavelength region and direct transmittance in the red-wavelength region. A rough surface is expected for the thicker FTO layer, resulting in an increase in the diffuse scattering and less reflection. The surface of the thick FTO might act as a textured surface.

## 4. Conclusions

We employed two different FTO-coated glass substrates to compare their substrate performance on CdTe cells: substrate A consisted of FTO ( $300$  nm)/  $\text{SiO}_2$  ( $24$  nm)/  $\text{SnO}_2$  ( $30$  nm)/ borosilicate glass  $2.2$  mm and substrate B consisted of FTO ( $700$  nm)/  $\text{SnO}_2$  ( $30$  nm)/ borosilicate glass ( $1.8$  mm). The total thickness was approximately  $2.5$  mm. The cell efficiency of the CdTe cell on substrate B was consistently higher than that of the CdTe cell on substrate A, mainly due to the increase in the

short-circuit current. The optical transmittance analysis showed that the total transmittance (direct transmittance + diffuse transmittance) through substrate B was higher in the blue wavelength region than that through substrate A, and in addition, the direct transmittance through substrate B was also higher than that through substrate A in the red wavelength region. The diffuse transmittance played a key role in the blue wavelength region, while the direct transmittance acted as a key role in the higher transmittance. It was evident that a rough surface is necessary to increase the transmittance in the blue wavelength region and a lower carrier concentration is necessary to increase the transmittance in the red wavelength region.

By replacing the Cu metal contact on CdTe with a Cu solution contact, the cell efficiency increased further. With the Cu solution contact,  $J_{sc}$ ,  $V_{oc}$ , and FF improved. In particular, the QE values across the entire spectrum increased. As a result, the cell efficiency increased from 12.4 to 15.1% with the introduction of the thicker FTO substrate and Cu contact using a Cu solution instead of Cu metal. In particular, the  $J_{sc}$  value in the CdTe cell with substrate B and the Cu solution contact increased from 22.4 to 26.1 mA/cm<sup>2</sup> compared to that in the CdTe cell with substrate B and the Cu metal contact.

Our experiment demonstrated that the substrate should have high diffuse optical transmittance in the blue wavelength region and high direct transmittance in the red wavelength region. This suggests that FTO with a rough surface or textured surface for high diffuse transmission in the blue wavelength region and with a good electron mobility with lower carrier concentration is necessary for the red wavelength region.

## Acknowledgments

This work was financially supported by the Korea Research Foundation through the Center for Inorganic Photovoltaic Materials (2014-001796) and by the Korean Ministry of Science and Technology through the Climate Change Research Hub of KAIST (N01150136).

## References

1. M. A. Green, K. Emery, Y. Hishikawa, W. Warta, E. D. Dunlop, Solar cell efficiency tables (Ver. 45), *Prog. Photovolt. Res. Appl.*, **23**, 1 (2015).
2. D. M. Meysing, C. A. Wolden, M. M. Griffith, H. Mahabaduge, J. Pankew, M. O. Reese, J. M. Burst, W. L. Rance, T. M. Barnes, Properties of reactively sputtered oxygenated cadmium sulfide (CdS:O) and their impact on CdTe solar cell performance, *J. Vacuum Sci. Technol. A*, **33**, 021203 (2015).
3. X. Wu, J. Zhou, A. Duda, J. C. Keane, T. A. Gessert, Y. Yan, R. Noufi, 13.9%-efficient CdTe polycrystalline thin-film solar cells with an infrared transmission of similar to 50%, *Prog. Photovolt.*, **14**, 471 (2006).
4. K. Jeyadheepan, M. Thamilselvan, K. Kim, J. Yi, C. Sanjeeviraja, Optoelectronic properties of R-F magnetron sputtered Cadmium Tin Oxide (Cd<sub>2</sub>SnO<sub>4</sub>) thin films for CdS/CdTe thin film solar cell applications, *J. Alloys Compounds*, **620**, 185 (2015).
5. M. S. Kim, L. Larina, J. H. Yun, B. T. Ahn, Fabrication of CdTe solar cell using an In(OOH,S)/CdS double layer as a heterojunction counterpart, *Curr. Appl. Phys.* **9**, 455 (2009).
6. E. S. Cha, Y. M. Ko, S. C. Kim, B. T. Ahn, Short-circuit current improvement in CdTe solar cells by combining a ZnO buffer and a solution back contact, *Curr. Appl. Phys.* **17**, 47-54 (2017).
7. C.J. D. Godines, C. G. T. Castanedo, CGT, R. C. Perez, G. T. Delgado, O. Z. Angel, Transparent conductive thin films of Cd<sub>2</sub>SnO<sub>4</sub> obtained by the sol-gel technique and their use in a solar cell made with CdTe, *Sol. Ener. Mater. Sol. Cel.*, **128**, 150-155, 2014.
8. S. Vatavu, C. Rotaru, V. Fedorov, T. A. Stein, M. Caraman, I. Evtodiev, C. Kelch, M. Kirsch, P. Chetrus, P. Gasin, ; Lux-Steiner, MC (Lux-Steiner, Martha Ch.)<sup>2</sup>; Rusu, M (Rusu, Marin)<sup>1,2</sup> A comparative study of (ZnO, In<sub>2</sub>O<sub>3</sub>: SnO<sub>2</sub>, SnO<sub>2</sub>)/CdS/CdTe/(Cu/Ni) heterojunctions, *Thin Solid Films*, **535**, 244-248 (2013).
9. J. Perrenoud, L. Kranz, S. Buecheler, F. Pianezzi, A. N. Tiwari, *Thin Solid Films*, The use of Al-doped ZnO as transparent conductive oxide for CdS/CdTe solar cells, **519**, 7444 (2011).
10. H. D. Kim, D.S. Kim, Kurn, Cgo, B. T. Ahn, H. B. Im, Photovoltaic Properties of Sintered CdS/CdTe solar cells with an indium-tin-oxide electrode, *J. Electrochem. Soc.*, **141**, 3572 (1994).
11. J. Britt, C. Ferekides, *Appl. Phys. Lett.*, Thin-film CdS/CdTe solar cell with 15.8% efficiency, **62**, 2851 (1993).
12. D. Grecu, A. D. Compaan, D. Young, U. Jayamaha and D. H. Rose, Photoluminescence of Cu-doped CdTe and related stability issues in CdS/CdTe solar cells, *J. Appl. Phys.* **88**, 2490 (2000).
13. I. Visoly-Fisher, K.D. Dobson, J. Nair, E. Bezalet, G. Hodes, D. Cahen, Factors affecting the stability of CdTe/CdS solar cells deduced from stress tests at elevated temperature, *Adv. Funct. Mater.* **13** (2003) 289 (2003).
14. B. A. Korevaar, R. Shuba, A. Yakimov, H. Cao, J. C. Rojo, T. R. Tolliver, Initial and degraded performance of thin film CdTe solar cell devices as a function of copper at the back contact, *Thin Solid Films*, **519**, 7160 (2011).
15. H. C. Chou, A. Rohatgi, E. W. Thomas, S. Kamra, A. K. Bhat,

- Effects of Cu on CdTe/CdS Heterojunction Solar Cells with Au/Cu Contacts, *J. Electrochem. Soc.*, **142**, 254 (1995).
16. B. T. Ahn, J. H. Yun, E. S. Cha, K. C. Park, Understanding the junction degradation mechanism in CdS/CdTe solar cells using a Cd-deficient CdTe layer, *Curr. Appl. Phys.*, **12**, **174** (2012).
  17. V. Evani, M. Khan; S. Collins, V. Palekis, P. Bane, D. Morel, C. Ferekides, Effect of Cu and Cl on EVT-CdTe solar cells, *Proc. 42<sup>nd</sup> Photovolt. Special. Conf. (PVSC)*, 1-5, New Orleans (2015).
  18. S. Demtsu and J. Sites, D. Albin, Role of Copper in the Performance of CdS/CdTe Solar Cells, *Proc. 4th World Conf. Photovolt. Energy Conv. (WCPEC-4)*, 523-529, Waikoloa (2006).